ОБЪЕДИНЕННЫЙ
ИНСТИТУТ
ЯДЕРНЫХ
ИССЛЕДОВАНИЙ

ДУБНА

29/XII-75

E2 - 9129

D.B.Ion

EXACT SATURATION AND DEGENERACY OF ISOSPIN BOUNDS AND ZEROS TRAJECTORIES IN PION-NUCLEON SCATTERING

1975

E2 - 9129

D.B.Ion*

EXACT SATURATION AND DEGENERACY OF ISOSPIN BOUNDS AND ZEROS TRAJECTORIES IN PION-NUCLEON SCATTERING

Submitted to Annals of Physics

* On leave of absence from Institute for Atomic Physics, Bucharest, Romania.

1. Introduction

The isospin constraints on differential observables of $(0^{-}1/2^{+} \to 0^{-}\,1/2^{+})$ reactions, which are more stronger than the usual triangular inequalities, were recently obtained in ref. [1-5]. A remarkable equality (see eq. (3), this paper) and the bound $4H \leq -\lambda(\sigma)$ were derived in ref. [1,2] while other equalities and bounds [see eqs. (4a,b), (5), (6) and (7a,b,d), this paper] were obtained in ref. [2-5]. The method of investigation of isospin bounds introduced in ref. [2,5] has the advantage that the exact saturation of isospin bounds can be expressed in terms of the zeros trajectories of imaginary part of a specific bilinear form. Thus, all the constraints on the scattering amplitudes, when the isospin bounds are exactly saturated or degenerated can be unambiguously established.

In this paper, the exact saturation and degeneracy of isospin bounds, in terms of the zero trajectories of imaginary parts of different bilinear forms, are investigated using the CERN-theoretical [6] and CERN-experimental [7] solutions for pion-nucleon phase shifts. So, in Sect. 2 we summarize the isospin constraints implied by the triangular relationship (1) on the differential observables of $(0^- \ 1/2^+ \to 0^- \ 1/2^+)$ reactions. In sect. 3 we discuss the exact saturation of isospin bounds in terms of $\mathrm{Im} N_{ij}$ -zeros trajectories $[N_{ij} \equiv M_{ij}^{(\pm\kappa)}, Z_{ij}^{(0)}, Z_{ij}^{(\kappa)}]$ obtained from the CERN-theoretic solution /6/ for πN -phase shifts. The degeneracy of isospin bounds or equivalently "phase degeneracy" is also investigated in sect. 3 by using the CERN-experimental solution /7/ for πN -phase shifts.

2. Isospin Constraints for $(0^- \ 1/2^+ \to 0^- \ 1/2^+)$ Reactions

Let us consider three $(0^- 1/2^+ \to 0^- \ 1/2^+)$ reactions related by the internal symmetries via two (isospin, U-spin, or V-spin, etc.) channels. Then the transition matrices T_i , $i = 1,2,3$, of these reactions satisfy the sum rule

$$\sum_{i=1}^{3} c_i T_i = 0, \qquad (1)$$

where c_i are given by products of Clebsh-Gordan coefficients. The coefficients c_i , for some usual reactions related by isospin invariance, are listed in table I (see also ref. /8,9/). In general, the test of the sum rule (1), at intermediate angles, is more involved due to spin complications. The full content of the triangular relationship (1) can only be used, if the spin rota-

Table I

The c_i -coefficients for some usual meson-baryon reactions

i	$\pi p \to \pi N$	c_i	i	$\pi p \to K\Sigma$	c_i
1	$\pi^+ p \to \pi^+ p$	+1	1	$\pi^+ p \to K^+ \Sigma^+$	+1
2	$\pi^- p \to \pi^- p$	-1	2	$\pi^- p \to K^+ \Sigma^-$	-1
3	$\pi^- p \to \pi^0 n$	$-\sqrt{2}$	3	$\pi^- p \to K^0 \Sigma^0$	$-\sqrt{2}$
i	$K p \to K N$	C_i	i	$\bar{K} p \to \bar{K} N$	C_i
1	$K^+ p \to K^+ p$	+1	1	$K^- p \to K^- p$	+1
2	$K^0 p \to K^0 p$	-1	2	$\bar{K}^0 p \to \bar{K}^0 p$	-1
3	$K^0 p \to K^+ n$	-1	3	$K^- p \to K^0 n$	-1
i	K_S^0-reggeneration on: proton	c_i	i	K_S^0-reggeneration on: neutron	c_i
1	$K^+ n \to K^+ n$	+1	1	$K^+ p \to K^+ p$	+1
2	$K^- n \to K^- n$	-1	2	$K^- p \to K^- p$	-1
3	$K_L^0 p \to K_S^0 p$	+2	3	$K_L^0 n \to K_S^0 n$	+2

tion vectors $\vec{P}_i$ for all the three reactions are known in addition to the differential cross-sections σ_i. Therefore a problem of great interest in obtaining the detailed test of isospin invariance (SU(3) -symmetry [8], quark models [9], etc.), when the experimental data with high statistics from the meson factories will become available, is to know all the constraints implied by the triangular relationship (1) on the experimental observables σ_i and $\vec{P}_i$, $i = 1, 2, 3$.
For this purpose we start with the following definitions:

$$\lambda(x, y, z) \equiv x^2 + y^2 + z^2 - 2xy - 2xz - 2yz\,, \tag{2a}$$

$$\lambda(\sigma) \equiv \lambda[\, c_1^2\sigma_1,\ c_2^2\sigma_2,\ c_3^2\sigma_3\,]\,, \tag{2b}$$

$$\lambda(\vec{\kappa}\cdot\vec{P}\sigma) \equiv \lambda[\, c_1^2\sigma_1\vec{\kappa}\cdot\vec{P}_1,\ c_2^2\sigma_2\vec{\kappa}\cdot\vec{P}_2,\ c_3^2\sigma_3\vec{\kappa}\cdot\vec{P}_3\,]\,, \tag{2c}$$

$$\lambda_\kappa^{(\pm)} \equiv \lambda[\, c_1^2\sigma_1(1 \pm \vec{\kappa}\cdot\vec{P}_1),\ c_2^2\sigma_2(1 \pm \vec{\kappa}\cdot\vec{P}_2),\ c_3^2\sigma_3(1 \pm \vec{\kappa}\cdot\vec{P}_3)\,]\,, \tag{2d}$$

$$H_{ij} \equiv \frac{1}{2}[\,1 - \vec{P}_i\cdot\vec{P}_j\,]\,\sigma_i\,\sigma_j\,, \tag{2e}$$

$$M_{\ell\ell}^{(\pm\kappa)} \equiv (1 \pm \vec{\kappa}\cdot\vec{P}_\ell)\,\sigma_\ell\,,\quad Z_{\ell\ell}^{(\kappa)} \equiv (\vec{\kappa}\cdot\vec{P}_\ell)\,\sigma_\ell\,,\quad \ell = 1,2,3\,, \tag{2f}$$

$$a_\kappa \equiv \frac{2[\sigma_i\sigma_j - H_{ij}]^{1/2}}{\sigma_i\sigma_j}\,[\, c_k^2 Z_{kk}^{(\kappa)} - c_i^2 Z_{ii}^{(\kappa)} - c_j^2 Z_{jj}^{(\kappa)}\,] - \frac{\vec{\kappa}\cdot(\vec{P}_i + \vec{P}_j)}{[\sigma_i\sigma_j - H_{ij}]^{1/2}}\,[\, c_k^2\sigma_k - c_i^2\sigma_i - c_j^2\sigma_j\,]\,, \tag{2g}$$

where the three indices $k \neq i \neq j$ represent any permutation of 1,2,3, $\vec{\kappa}$ is an arbitrary unit vector in the spin space. Then, all the constraints implied by the sum rule (1) may be conveniently summarized as follows. <u>The sum rule (1) alone implies that the unpolarized differential cross-sections σ_ℓ and spin rotation vectors P_ℓ, $\ell = 1,2,3$ must obey the equalities:</u>

$$H \equiv c_1^2 c_2^2 H_{12} = c_2^2 c_3^2 H_{23} = c_3^2 c_1^2 H_{31} \geq 0\,, \tag{3}$$

$$\frac{1}{2}\,|\,\lambda_\kappa^{(+)} - \lambda_\kappa^{(-)}\,| = 2\,[-4H - \lambda(\sigma)]^{1/2}\,[4H - \lambda(\vec{\kappa}\cdot\vec{P}\sigma)]^{1/2}\,, \tag{4a}$$

$$|\,2H + \frac{1}{4}\lambda(\sigma) - \frac{1}{4}\lambda(\vec{\kappa}\cdot\vec{P}\sigma)\,| = [-\frac{1}{4}\lambda_\kappa^{(+)}]^{1/2}\,[-\frac{1}{4}\lambda_\kappa^{(-)}]^{1/2}\,, \tag{4b}$$

[see also eqs. (4c,d) from ref. [4]],

$$\begin{aligned}
&4H[\, c_k^2 M_{kk}^{(+\kappa)} - c_i^2 M_{ii}^{(+\kappa)} - c_j^2 M_{jj}^{(+\kappa)}\,][\, c_k^2 M_{kk}^{(-\kappa)} - c_i^2 M_{ii}^{(-\kappa)} - c_j^2 M_{jj}^{(-\kappa)}\,] - \\
&- 4c_i^4 c_j^4 \sigma_i^2 \sigma_j^2 [\vec{\kappa}\cdot(\vec{P}_i \times \vec{P}_j)]^2 = \lambda(\sigma)\,[\, c_k^2 Z_{kk}^{(\kappa)} - c_i^2 Z_{ii}^{(\kappa)} - c_j^2 Z_{jj}^{(\kappa)}\,]^2 + \\
&+ \lambda(\vec{\kappa}\cdot\vec{P}\sigma)\,[\, c_k^2\sigma_k - c_i^2\sigma_i - c_j^2\sigma_j\,]^2 + \\
&+ \frac{1}{2}[-\lambda_\kappa^{(+)} + \lambda_\kappa^{(-)}\,][\, c_k^2 Z_{kk}^{(\kappa)} - c_i^2 Z_{ii}^{(\kappa)} - c_j^2 Z_{jj}^{(\kappa)}\,][\, c_k^2\sigma_k - c_i^2\sigma_i - c_j^2\sigma_j\,],
\end{aligned} \tag{5}$$

$$\frac{a_{\kappa'}}{a_{\kappa''}} = \frac{\vec{\kappa}'\cdot(\vec{P}_i \times \vec{P}_j)}{\vec{\kappa}''\cdot(\vec{P}_i \times \vec{P}_j)} \quad \text{for any } \vec{\kappa}' \text{ and } \vec{\kappa}'', \tag{6}$$

and the bounds

$$0 \le -\lambda_{\kappa}^{(\pm)} \le \min_{[ij]} \{ c_i^2 c_j^2 \sigma_i \sigma_j (1 \pm \vec{\kappa}\cdot\vec{P}_i)(1 \pm \vec{\kappa}\cdot\vec{P}_j) \}, \tag{7a}$$

$$4 \max_{[ij]} \{ c_i^2 c_j^2 (\vec{\kappa}\cdot\vec{P}_i)(\vec{\kappa}\cdot\vec{P}_j)\sigma_i \sigma_j \} \le \lambda(\vec{\kappa}\cdot\vec{P}\sigma) \le 4H, \tag{7b}$$

$$4H \le -\lambda(\sigma) \le 4\cdot \min_{[ij]} \{ c_i^2 c_j^2 \sigma_i \sigma_j \}, \tag{7c}$$

$$\Omega_{\kappa}^{(-)} \le H \le \Omega_{\kappa}^{(+)}, \tag{7d}$$

$$\Omega_{\kappa}^{(\pm)} \equiv \frac{1}{2} \left[\begin{matrix}\min \\ \max\end{matrix} \right]_{\{ij\}} \{ c_i^2 c_j^2 [1 - (\vec{\kappa}\cdot\vec{P}_i)(\vec{\kappa}\cdot\vec{P}_j) \pm \\ \pm [1 - (\vec{\kappa}\cdot\vec{P}_i)^2]^{1/2} [1 - (\vec{\kappa}\cdot\vec{P}_j)^2]^{1/2}] \}, \tag{7d'}$$

at any energy and all scattering angles for any unit vector $\vec{\kappa}$ in any spin reference frame.

The constraints (3) and (7c) were introduced in ref. /1,2/ while the equalities (4a,b), (5), (6) and the bounds (7a,b,d) were derived recently in ref. /3-5/ . The lower bounds (7a) were also remarked by Tornqvist et al. /10/ as a generalization of the usual triangular inequalities /11-12/ on polarizations and spin-rotation parameters (A, R). In ref. /4/ we have proved that eq. (3) and the bounds (7a,b,c,d) are also valid for the integrated cross-sections and average spin-rotation vectors.

Next, using eqs. (3), (5) and (6) it is easy to see that the test quantity H [see eq. (3) and (2d)] and the spin rotation parameters A_k , R_k and R_j can be expressed in terms of σ_i , σ_j , σ_k , P_i , P_j , P_k , A_i , R_i and A_j , $i \ne j \ne k$ by the following relations:

$$H = \frac{B_P + D_{AP}}{\gamma_P - 16 c_i^2 c_j^2 \sigma_i \sigma_j A_i A_j}, \tag{8a}$$

$$A_k = \frac{\alpha_{AP}}{c_k^2 \sigma_k} [c_k^2 (P_k - \beta_P)\sigma_k - c_i^2 (P_i - \beta_P)\sigma_i - c_j^2 (P_j - \beta_P)\sigma_j] + \\ + \beta_A + \frac{c_i^2 \sigma_i}{c_k^2 \sigma_k}(A_i - \beta_A) + \frac{c_j^2 \sigma_j}{c_k^2 \sigma_k}(A_j - \beta_A), \tag{8b}$$

$$R_m = \frac{c_i^2 c_m^2 [1 - P_j P_m - A_j A_m] \sigma_j \sigma_m - 2H}{c_i^2 c_j^2 [1 - P_j P_i - A_j A_i] \sigma_j \sigma_i - 2H} R_i, \tag{8c}$$

$m = j, k$

where

$$B_P \equiv \lambda(\sigma)\,[c_k^2\sigma_k P_k - c_i^2\sigma_i P_i - c_j^2\sigma_j P_j]^2 + \lambda(P\sigma)[c_k^2\sigma_k - c_i^2\sigma_i - c_j^2\sigma_j]^2 +$$

$$+ \frac{1}{2}[-\lambda_P^{(+)} + \lambda_P^{(-)}][c_k^2\sigma_k P_k - c_i^2\sigma_i P_i - c_j^2\sigma_j P_j][c_k^2\sigma_k - c_i^2\sigma_i - \qquad (8d)$$

$$- c_j^2\sigma_j],$$

$$\lambda_P^{(\pm)} \equiv \lambda\,[c_1^2\sigma_1(1 \pm P_1),\ c_2^2\sigma_2(1 \pm P_2),\ c_3^2\sigma_3(1 \pm P_3)], \qquad (8e)$$

$$D_{AP} \equiv 4\,c_i^4 c_j^4 \sigma_i^2\sigma_j^2\,[(A_i - A_j)^2 - (A_i P_j - A_j P_i)^2], \qquad (8f)$$

$$\gamma_P \equiv 4[c_k^2\sigma_k(1 + P_k) - c_i^2\sigma_i(1 + P_i) - c_j^2(1 + P_j)\sigma_j] \times \qquad (8g)$$
$$\times [c_k^2\sigma_k(1 - P_k) - c_i^2\sigma_i(1 - P_i) - c_j^2\sigma_j(1 - P_j)],$$

$$a_{AP} \equiv \frac{c_i^2 c_j^2 \sigma_i \sigma_j [P_j - P_i + A_j(P_i A_j - P_j A_i)] - 2HP_j}{c_i^2 c_j^2 \sigma_i \sigma_j [A_i - A_j + P_j(P_i A_j - P_j A_i)] + 2HA_j}, \qquad (8h)$$

$$\beta_X \equiv \frac{c_i^2 c_j^2 \sigma_i \sigma_j (X_i + X_j)}{2[c_i^2 c_j^2 \sigma_i \sigma_j - H]}. \qquad (8i)$$

Therefore, as we can see from eq. (4b), the test quantity H can, up to a two-fold ambiguity, be expressed only in terms of σ_i, σ_j, σ_k, P_i, P_j, P_k. H is uniquely determined [see eq. (8a)] if also two spin rotation parameters are known [e.g., A_i and A_j]. Hence, if the experimental data on σ_i, σ_j, σ_k, P_i, P_j, P_k, A_i (or R_i) A_j (or R_j) are available, eqs. (4a,b) can be used to obtain certain tests of the sum rule (1). We note, of course, that a detailed test of isospin sum rule (1) can be obtained only if complete and accurate experimental data for all the three reactions are available.

3. Saturation of Isospin Bounds and Phase Contours

As we have mentioned in sect. 1, the method of investigation of isospin bounds introduced in ref. [2-5] has the advantage that the exact saturation of isospin bounds can be expressed in terms of the zeros trajectories of imaginary part of a specific bilinear form. Indeed, let f_ℓ and g_ℓ be the usual spin-non-flip and spin-flip scattering amplitudes and let $F_\ell^{(\pm\kappa)}$ be the following combinations of the scattering amplitudes:

$$F_\ell^{(+\kappa)} \equiv \frac{\sqrt{2}}{[1 + |w|^2]^{1/2}}[f_\ell + w g_\ell],$$

$$F_\ell^{(-\kappa)} \equiv \frac{\sqrt{2}}{[1 + |w|^2]^{1/2}}[-w^* f_k + g_k], \qquad (9a)$$

where w is an arbitrary complex number.
If we define the bilinear forms

$$M_{ij}^{(\pm\kappa)} = [F_i^{(\pm\kappa)}]^* F_j^{(\pm\kappa)} , \tag{9b}$$

and

$$Z_{ij}^{(0)} = \frac{1}{2}[M_{ij}^{(+\kappa)} + M_{ij}^{(-\kappa)}] , \quad Z_{ij}^{(\kappa)} = \frac{1}{2}[M_{ij}^{(+\kappa)} - M_{ij}^{(-\kappa)}] , \tag{9c}$$

then, the isospin sum rule (1) alone implies (see ref. /4/)

$$c_i^2 c_j^2 [\mathrm{Im}\, M_{ij}^{(\pm\kappa)}]^2 = -\frac{1}{4}\lambda_\kappa^{(\pm)} = \{[-H - \frac{1}{4}\lambda(\sigma)]^{1/2} \pm \eta_\kappa [H - \frac{1}{4}\lambda(\vec{\kappa}\cdot\vec{P}\sigma)]^{1/2}\}^2 ; \tag{10a}$$

$$c_i^2 c_j^2 [\mathrm{Im}\, Z_{ij}^{(0)}]^2 = -H - \frac{1}{4}\lambda(\sigma) = \frac{1}{4}\{[-\frac{1}{4}\lambda_\kappa^{(+)}]^{1/2} + \epsilon_\kappa [-\frac{1}{4}\lambda_\kappa^{(-)}]^{1/2}\}^2 ; \tag{10b}$$

$$c_i^2 c_j^2 [\mathrm{Im}\, Z_{ij}^{(\kappa)}]^2 = H - \lambda(\vec{\kappa}\cdot\vec{P}\sigma) = \frac{1}{4}\{[-\frac{1}{4}\lambda_\kappa^{(+)}]^{1/2} - \epsilon_\kappa [-\frac{1}{4}\lambda_\kappa^{(-)}]^{1/2}\}^2 ; \tag{10c}$$

where

$$\eta_\kappa \equiv \mathrm{sign}\,[\mathrm{Im}\, Z_{ij}^{(0)}\, \mathrm{Im}\, Z_{ij}^{(\kappa)}] = \mathrm{sign}\,\{-\lambda_\kappa^{(+)} + \lambda_\kappa^{(-)}\} , \tag{10d}$$

$$\epsilon_\kappa \equiv \mathrm{sign}\,[\mathrm{Im}\, M_{ij}^{(+\kappa)}\, \mathrm{Im}\, M_{ij}^{(-\kappa)}] = \mathrm{sign}\,\{-8H - \lambda(\sigma) + \lambda(\vec{\kappa}\cdot\vec{P}\sigma)\}. \tag{10e}$$

Therefore, the positivity conditions $[\mathrm{Im}\, N_{ij}]^2 \geq 0$, for $N_{ij} \equiv M_{ij}^{(\pm\kappa)}$, $Z_{ij}^{(0)}$ and $Z_{ij}^{(\kappa)}$ imply the lower bounds (7a,c) and the upper bound (7b), respectively.
Hence, the isospin bounds

$$-\lambda_\kappa^{(\pm)} \geq 0, \tag{11a}$$

$$4H \leq -\lambda(\sigma), \tag{11b}$$

$$\lambda(\vec{\kappa}\cdot\vec{P}\sigma) \leq 4H , \tag{11c}$$

are exactly saturated on the zeros trajectories of the imaginary part of the bilinear forms $M_{ij}^{(\pm\kappa)}$, $Z_{ij}^{(0)}$ and $Z_{ij}^{(\kappa)}$, respectively.

Next, let $\delta_{ij}^{(\pm\kappa)}$, $\phi_{ij}^{(0)}$ and $\phi_{ij}^{(\kappa)}$ be the phases corresponding to the bilinear forms $M_{ij}^{(\pm\kappa)}$, $Z_{ij}^{(0)}$ and $Z_{ij}^{(\kappa)}$, respectively. Then, the isospin sum rule (1) implies that all these phases are experimentally observable.

Indeed, $\cos\delta_{ij}^{(\pm\kappa)}$, $\cos\phi_{ij}^{(0)}$ and $\cos\phi_{ij}^{(\kappa)}$ can be determined from the relation

$$2c_i c_j \mathrm{Re}\, N_{ij} = c_k^2 N_{kk} - c_j^2 N_{jj} - c_i^2 N_{ii}, \qquad (12a)$$

obtained from the isospin sum rule (1) alone for each

$$N_{ij} \equiv M_{ij}^{(\pm\kappa)},\ Z_{ij}^{(0)},\ Z_{ij}^{(\kappa)}$$

since

$$M_{\ell\ell}^{(\pm\kappa)} = (1 \pm \vec{\kappa}\cdot\vec{P}_\ell)\sigma_\ell,\ Z_{\ell\ell}^{(0)} = \sigma_\ell,\ Z_{\ell\ell}^{(\kappa)} = \vec{\kappa}\cdot\vec{P}_\ell\ \sigma_\ell$$

and

$$|M_{ij}^{(\pm\kappa)}|^2 = M_{ii}^{(\pm\kappa)} M_{jj}^{(\pm\kappa)},$$

$$|Z_{ij}^{(0)}|^2 = \frac{1}{2}(1 + \vec{P}_i\cdot\vec{P}_j)\sigma_i\sigma_j, \qquad (12b)$$

$$|Z_{ij}^{(\kappa)}|^2 = H_{ij} + Z_{ii}^{(\kappa)} Z_{jj}^{(\kappa)},$$

where H_{ij} is defined by eq. (2d). The sign of $\sin\delta_{ij}^{(\pm\kappa)}$, $\sin\phi_{ij}^{(0)}$ and $\sin\phi_{ij}^{(\kappa)}$ can be obtained as follows. According to the relation

$$Z_{ij}^{(0)}[Z_{ij}^{(\kappa)}]^* = \frac{\sigma_i\sigma_j}{2}\{\vec{\kappa}\cdot(\vec{P}_i + \vec{P}_j) + i\vec{\kappa}\cdot(\vec{P}_i \times \vec{P}_j)\}, \qquad (13a)$$

we obtain

$$\mathrm{Re}\, Z_{ij}^{(\kappa)} = \frac{\sigma_i\sigma_j}{2|Z_{ij}^{(0)}|}\{\vec{\kappa}\cdot(\vec{P}_i + \vec{P}_j)\cos\phi_{ij}^{(0)} + \vec{\kappa}\cdot(\vec{P}_i \times \vec{P}_j)\sin\phi_{ij}^{(0)}\} \qquad (13b)$$

and

$$\mathrm{Im}\, Z_{ij}^{(\kappa)} = \frac{\sigma_i\sigma_j}{2|Z_{ij}^{(0)}|}\{\vec{\kappa}\cdot(\vec{P}_i + \vec{P}_j)\sin\phi_{ij}^{(0)} - \vec{\kappa}\cdot(\vec{P}_i \times \vec{P}_j)\cos\phi_{ij}^{(0)}\}. \qquad (13c)$$

Then, from (12a) for $N_{ij} \equiv Z_{ij}^{(\kappa)}$ and (13b), we get

$$c_k^2\sigma_k\vec{P}_k - c_i^2\sigma_i\vec{P}_i - c_j^2\sigma_j\vec{P}_j = \qquad (14)$$
$$= \frac{c_i c_j \sigma_i \sigma_j}{|Z_{ij}^{(0)}|}\{(\vec{P}_i + \vec{P}_j)\cos\phi_{ij}^{(0)} + (\vec{P}_i \times \vec{P}_j)\sin\phi_{ij}^{(0)}\},$$

Hence,

$$\mathrm{sign}[\sin\phi_{ij}^{(0)}] = \mathrm{sign}[\vec{P}_k\cdot(\vec{P}_i\times P_j)], \qquad (15)$$

while the sign of $\sin\phi_{ij}^{(\kappa)}$ and $\sin\delta_{ij}^{(\pm\kappa)}$ can be determined using eqs. (13c) and $\mathrm{Im}\,M_{ij}^{(\pm\kappa)} = \mathrm{Im}Z_{ij}^{(0)} \pm \mathrm{Im}\,Z_{ij}^{(\kappa)}$. We note that eqs. (14) and (15) are equivalent to eqs. (27) and (29) fro, ref. /1/ . Also, we remark that nine experimental observables [e.g., σ_i, σ_j, σ_k, P_i, P_j, P_k, A_i, A_j, $\mathrm{sign}(R_i)$] are sufficient to determine uniquely all the phases: $\delta_{ij}^{(\pm\kappa)}$, $\phi_{ij}^{(0)}$ and $\phi_{ij}^{(\kappa)}$, since as we have seen in sect. 2, three spin rotation parameters can be expressed in terms of nine experimental quantities [see, for example, eqs. (8b,c)]. Therefore, if we define a $[\delta_{ij}^{(\pm\kappa)}, \phi_{ij}^{(0)}, \phi'^{(\kappa)}_{ij}]$-phase contour as the curve on which the phase of the corresponding bilinear form takes a given constant (real) value, then the isospin bounds (11a,b,c) are exactly saturated on the $[\delta_{ij}^{(\pm\kappa)}, \phi_{ij}^{(0)}, \phi_{ij}^{(\kappa)}] = n\pi$ -phase contours, respectively. The upper bounds (7a,c) and the lower bound (7b) are exactly saturated on the

$$[\delta_{ij}^{(\pm\kappa)}, \phi_{ij}^{(0)}, \phi_{ij}^{(\kappa)}] = (n+\tfrac{1}{2})\pi \text{ -phase contours } (n = 0\ 1, \ldots,).$$

The bounds (7a,b,c) are degenerated if and only if $|N_{ij}| = 0$ for $N_{ij} \equiv M_{ij}^{(\pm\kappa)}, Z_{ij}^{(\kappa)}, Z_{ij}^{(0)}$, respectively. Then, the phase of the corresponding bilinear form is not determined. We note, of course, that $[\delta_{ij}^{(\pm\kappa)}, \phi_{ij}^{(0)}, \phi_{ij}^{(\kappa)}] = n\pi$ phase contours lie on

$[\mathrm{Im}M_{ij}^{(\pm\kappa)}, \mathrm{Im}Z_{ij}^{(0)}, \mathrm{Im}Z_{ij}^{(\kappa)}]$ - zeros trajectories while $[\delta_{ij}^{(\pm\kappa)}, \phi_{ij}^{(0)}, \phi_{ij}^{(\kappa)}] = (n+\frac{1}{2})\pi$ - phase contours lie on $[\mathrm{Re}M_{ij}^{(\pm\kappa)}, \mathrm{Re}Z_{ij}^{(0)}, \mathrm{Re}Z_{ij}^{(\kappa)}]$ - zeros trajectories.

In general the $[\delta_{ij}^{(\pm\kappa)}, \phi_{ij}^{(0)}, \phi_{ij}^{(\kappa)}] = n\pi$ and $(n+\frac{1}{2})\pi$ phase contours have remarkable properties such as: (i) they are simply related to the resonance poles and zeros of different scattering amplitudes see ref. /2/, (ii) these are closely related to the strong constraints (implied by isospin invariance) on the (polarization) experimental data and also to the interference and isospin breaking phenomena, etc. The contraints on the experimental data corresponding to each $[\delta_{ij}^{(\pm\kappa)}, \phi_{ij}^{(0)}, \phi_{ij}^{(\kappa)}] = n\pi$ and $(n+\frac{1}{2})\pi$ phase contours are presented in Table II. The main reason for a systematic study of these phase contours is that it provides a new and interesting way to looking at the characteristis properties of scattering amplitudes. The phase contour diagram provides a convenient picture for the comparison of the scattering amplitudes which are obtained from specific asymptotic assumptions or by different phenomenological amplitude analyses. In particular the $[\mathrm{Im}M_{ij}^{(\pm\kappa)}, \mathrm{Im}Z_{ij}^{(0)}, \mathrm{Im}Z_{ij}^{(\kappa)}]$ zeros trajectories provide a graphic description of those properties of reactions which are independent of charge or (s,t,u) -isospin exchange channels [crossing invariant] since according to eqs. (10a,b,c) these zeros tra-

Table II

The constraints on experimental data corresponding to $[\delta_{ij}^{(\pm\kappa)}, \phi_{ij}^{(0)}, \phi_{ij}^{(\kappa)}] = n\pi$ and $(n+\frac{1}{2})\pi$ phase contours

Phase contours		Constraints on the experimental data
$\delta_{ij}^{(\pm\kappa)}$	$n\pi$	$\lambda_\kappa = 0$
	$(n+\frac{1}{2})\pi$	$c_k^2\sigma_k(1 \pm \vec{\kappa}\cdot\vec{P}_k) = c_i^2\sigma_i(1 \pm \vec{\kappa}\cdot\vec{P}_i) + c_j^2\sigma_j(1 \pm \vec{\kappa}\cdot\vec{P}_j)$
$\phi_{ij}^{(0)}$	$n\pi$	$c_i^2\sigma_i\vec{P}\,[c_i^2\sigma_i - c_j^2\sigma_j - c_k^2\sigma_k] + c_j^2\sigma_j\vec{P}_j[c_j^2\sigma_j - c_i^2\sigma_i - c_k^2\sigma_k] + c_k^2\sigma_k\vec{P}_k[c_k^2\sigma_k - c_i^2\sigma_i - c_j^2\sigma_j] = 0$
	$(n+\frac{1}{2})\pi$	$c_k^2\sigma_k = c_i^2\sigma_i + c_j^2\sigma_j$
$\phi_{ij}^{(\kappa)}$	$n\pi$	$c_i^2\sigma_i\,\vec{\kappa}\cdot\vec{P}_i[c_i^2\sigma_i - c_j^2\sigma_j - c_k^2\sigma_k] + c_j^2\sigma_j\,\vec{\kappa}\cdot\vec{P}_j[c_j^2\sigma_j - c_i^2\sigma_i - c_k^2\sigma_k] + c_k^2\sigma_k\,\vec{\kappa}\cdot\vec{P}_k[c_k^2\sigma_k - c_i^2\sigma_i - c_j^2\sigma_j] = 0$
	$(n+\frac{1}{2})\pi$	$c_k^2\sigma_k\,\vec{\kappa}\cdot\vec{P}_k = c_i^2\sigma_i\,\vec{\kappa}\cdot\vec{P}_i + c_j^2\sigma_j\,\vec{\kappa}\cdot\vec{P}_j$

jectories are all independent of change or isospin indices i,j. Also, we note that the zeros trajectories of $\mathrm{Im}Z_{ij}^{(0)}$ are invariant under rotations of the spin reference frame. Hence, it appears that these zeros trajectories can be used as a guide in developing a unified phenomenological theory that includes all the transfer momenta in both the low and medium energy regions as well as in the high energy regions. Therefore, it is of practical interest to obtain the $[\mathrm{Im}M_{ij}^{(\pm\kappa)}, \mathrm{Im}Z_{ij}^{(0)}, \mathrm{Im}Z_{ij}^{(\kappa)}]$ -zeros trajectories (for some particular $\vec{\kappa}$) from the available amplitude analyses.

Our results on the zeros trajectories of $\mathrm{Im}N_{ij}$, $N_{ij} \equiv M_{ij}^{(\pm\kappa)}, Z_{ij}^{(0)}, Z_{ij}^{(\kappa)}$, when $\vec{\kappa}$ is choosen such that $\vec{\kappa}\cdot\vec{P} = \mathbf{P}, \mathbf{T}, \mathbf{S}$ and $(\mathbf{A}, \mathbf{R})$ [see the definitions (2) from ref. /2/] obtained from the CERN theoretic phase shift solutions /6/ for the pion-nucleon scattering, are presented in figs. 1-5. We note that the bilinear forms $M_{ij}^{(\pm\kappa)}$ and $Z_{ij}^{(\kappa)}$ for $\vec{\kappa}\cdot\vec{P} = \mathbf{P}, \mathbf{T}, \mathbf{S}$ respectively, are obtained from eqs. (9a,b,c) for $w = i, 1, 0$ (resp.). Then we observe that these bilinear forms are identical with $M_{ij}^{(\pm n)}$ and $Z_{ij}^{(n)}$, $n = 1,2,3$ (resp.) defined in ref. /3/ by eqs. (1a,b,c). The bilinear forms for $\vec{\kappa}\cdot\vec{P} = \mathbf{A}, \mathbf{R}$ (resp.) are obtained in a similar way (using the helicity amplitudes). The bilinear forms $Z_{ij}^{(0)}$ are independent of $\vec{\kappa}$ since, according to eqs. (9a,b,c), we get

$$M_{ij}^{(+\kappa)} + M_{ij}^{(-\kappa)} = M_{ij}^{(+\kappa')} + M_{ij}^{(-\kappa')} = 2f_i^* f_j + 2g_i^* g_j \equiv 2Z_{ij}^{(0)}$$

for any $\vec{\kappa}$ and $\vec{\kappa}'$.

Therefore, from figs. 1-5, we see that the isospin bounds (11a,b,c) for $\vec{\kappa}\cdot\vec{P} = P, S, T, A$ and R (resp.) are exactly saturated along certain lines in the $[p_{LAB}, \cos\theta]$ -plane [here θ is the angle in the centre of mass] on the zeros trajectories of the imaginary parts of the corresponding bilinear forms $[M^{(\pm\kappa)}_{ij}, Z^{(0)}_{ij}, Z^{(\kappa)}_{ij}]$ . . On these lines the strong constraints on polarization experimental data and on amplitude analyses are imposed [see the constraints corresponding to $n\pi$ -phase contours from table II] . Next, it is easy to see that each pair of $[\mathrm{Im}M^{(+\kappa)}_{ij}, \mathrm{Im}M^{(-\kappa)}_{ij}]$ $[\mathrm{Im}Z^{(0)}_{ij}, \mathrm{Im}Z^{(\kappa)}_{ij}]$ - zeros trajectories are lines of exact saturation of the stringent bounds [see ref./4/]

$$2[-4H - \lambda(\sigma)]^{1/2}[4H - \lambda(\vec{\kappa}\cdot\vec{P}\sigma)]^{1/2} \le -\lambda(\sigma)-\lambda(\vec{\kappa}\cdot\vec{P}\sigma), \quad (16a)$$

and

$$[-\lambda^{(+)}_{\kappa}]^{1/2}[-\lambda^{(-)}_{\kappa}]^{1/2} \le -\lambda(\sigma) - \lambda(\vec{\kappa}\cdot\vec{P}\sigma), \quad (16b)$$

respectively, while all four $[\mathrm{Im}M^{(+\kappa)}_{ij}, \mathrm{Im}M^{(-\kappa)}_{ij}, \mathrm{Im}Z^{(0)}_{ij}, \mathrm{Im}Z^{(\kappa)}_{ij}]$ zeros trajectories are the lines of the exact saturation of the bound

$$B_{\kappa} \le -\lambda(\sigma) - \lambda(\vec{\kappa}\cdot\vec{P}\sigma), \quad (17a)$$

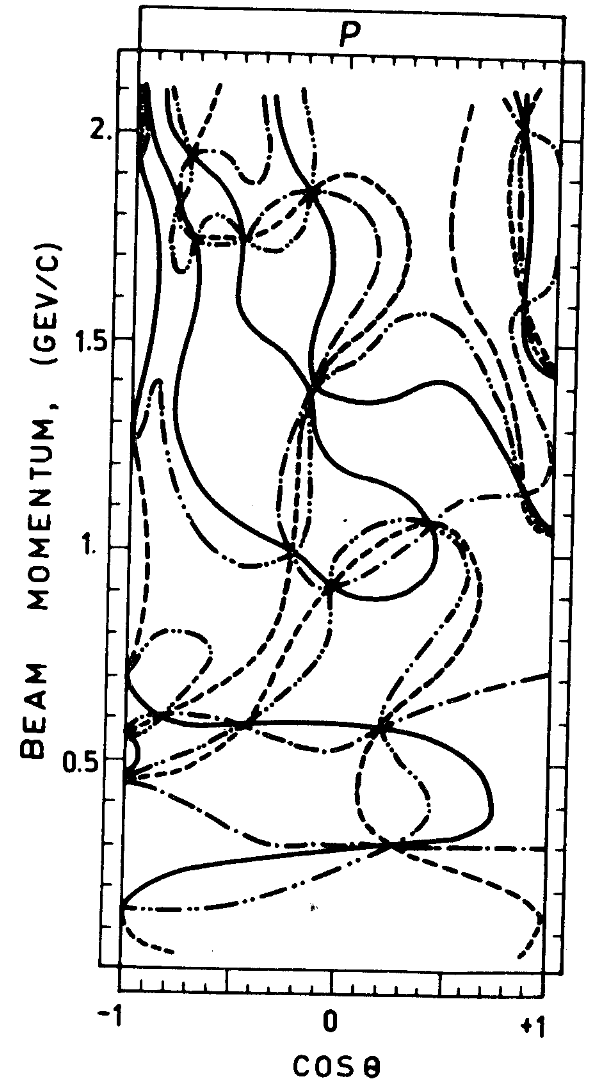

Fig. 1. The zeros trajectories of: $\mathrm{Im}M^{(+\kappa)}_{ij}$ (——), $\mathrm{Im}M^{(-\kappa)}_{ij}$ (- - - - -) , $\mathrm{Im}Z^{(\kappa)}_{ij}$ (-.-.-.-.) , $\mathrm{Im}Z^{(0)}_{ij}$ (-..-..-..-) , for $\vec{\kappa}\cdot\vec{P} = P$, determined from CERN theoretic solutions /6/ for πN -phase shifts.

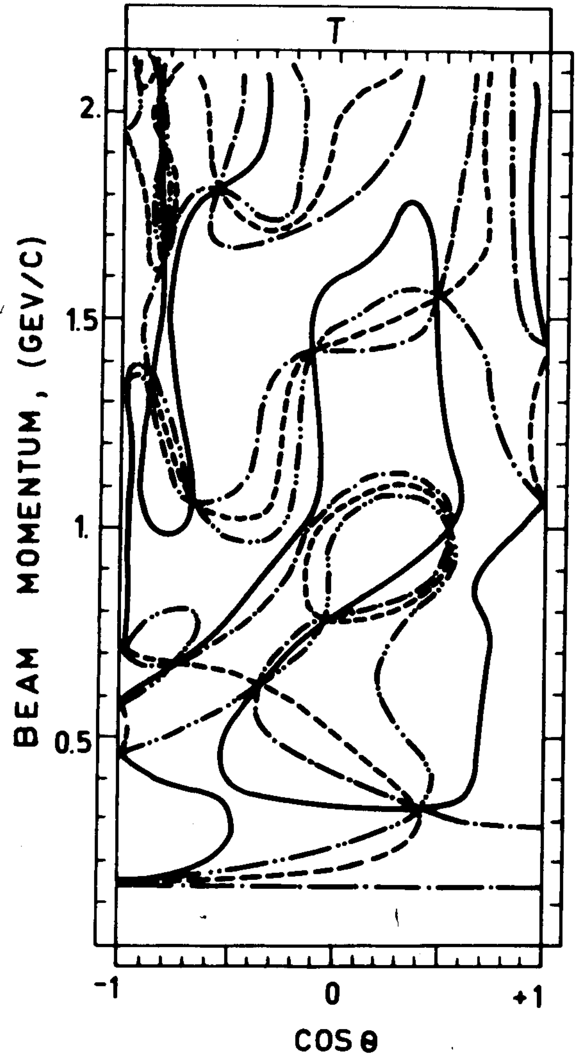

Fig. 2. The zeros trajectories of: $\mathrm{Im}\,M_{ij}^{(+\kappa)}$ (——), $\mathrm{Im}\,M_{ij}^{(-\kappa)}$ (– – – – – –) , $\mathrm{Im}\,Z_{ij}^{(\kappa)}$ (–·–·–·–·) , $\mathrm{Im}\,Z_{ij}^{(0)}$ (–··–··–) , for $\vec{\kappa}\cdot\vec{P} = T$, determined from CERN theoretic solutions /6/ for πN -phase shifts.

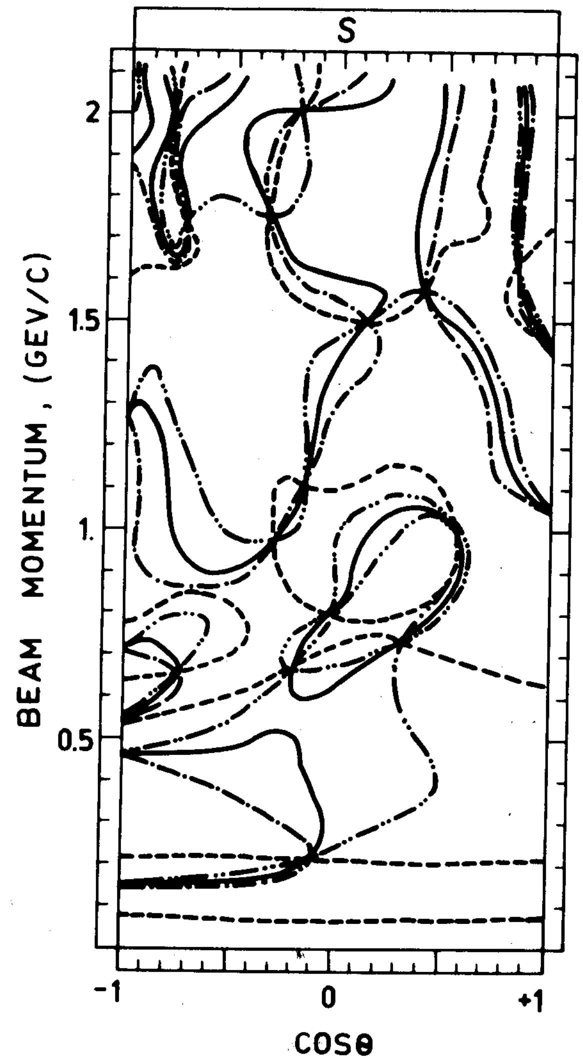

Fig. 3. The zeros trajectories of: $\mathrm{Im}\,M_{ij}^{(+\kappa)}$ (——), $\mathrm{Im}\,M_{ij}^{(-\kappa)}$ (– – – – –) , $\mathrm{Im}\,Z_{ij}^{(\kappa)}$ (–·–·–·–·) , $\mathrm{Im}\,Z_{ij}^{(0)}$ (–··–··–) , for $\vec{\kappa}\cdot\vec{P} = S$, determined from CERN theoretic solutions /6/ for πN -phase shifts.

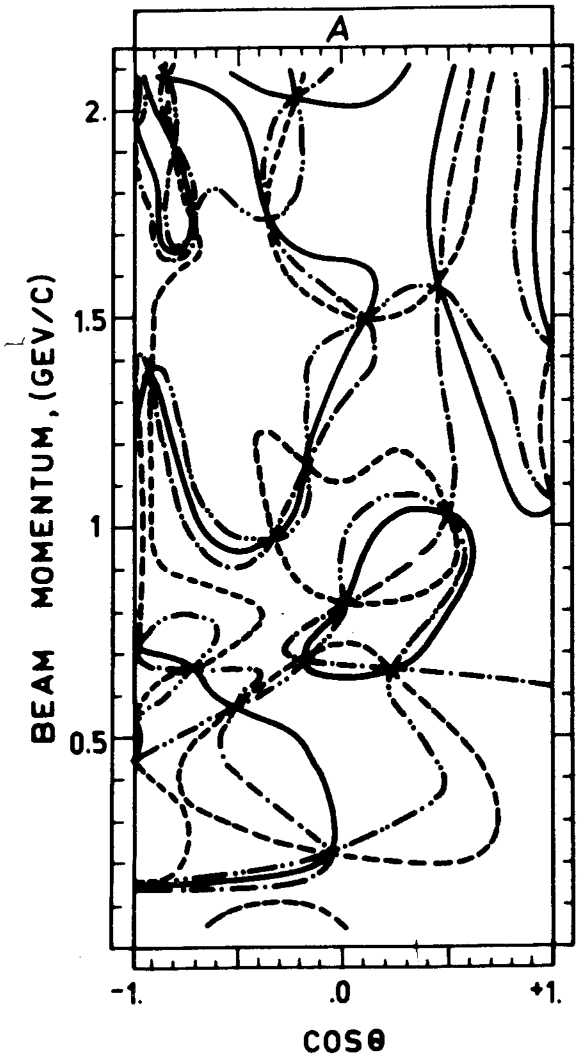

Fig. 4. The zeros trajectories of: $\mathrm{Im}M_{ij}^{(+\kappa)}$ (——), $\mathrm{Im}M_{ij}^{(-\kappa)}$ (– – – – –), $\mathrm{Im}Z_{ij}^{(\kappa)}$ (–·–·–·), $\mathrm{Im}Z_{ij}^{(0)}$ (–··–··–), for $\vec{\kappa}\cdot\vec{P} = A$, determined from CERN theoretic solutions /6/ for πN-phase shifts.

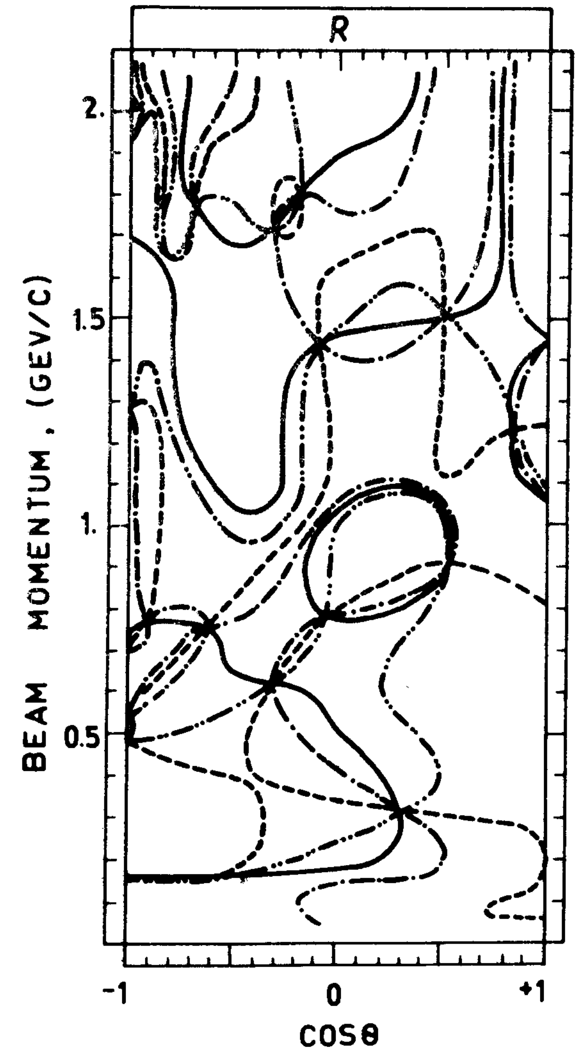

Fig. 5. The zeros trajectories of: $\mathrm{Im}M_{ij}^{(+\kappa)}$ (——), $\mathrm{Im}M_{ij}^{(-\kappa)}$ (– – – – –), $\mathrm{Im}Z_{ij}^{(\kappa)}$ (–·–·–·–·), $\mathrm{Im}Z_{ij}^{(0)}$ (–··–··–), for $\vec{\kappa}\cdot\vec{P} = R$, determined from CERN theoretic solutions /6/ for πN-phase shifts.

where

$$B_\kappa = \max\{[-\lambda_\kappa^{(+)}]^{1/2} \quad [-\lambda_\kappa^{(-)}]^{1/2}, 2[-4H-\lambda(\sigma)]^{1/2} \quad [4H-\lambda(\vec{\kappa}\cdot\vec{P}\sigma)]^{1/2}\}. \tag{17b}$$

The topology of the zeros trajectories [ZT] of $[\mathrm{Im}M_{ij}^{(\pm\kappa)}, \quad , \mathrm{Im}Z_{ij}^{(0)}, \quad \mathrm{Im}Z_{ij}^{(\kappa)}]$ presented in figs. 1-5, has some important aspects such as: (i) the zeros trajectories are intersected at certain points in the $[p_{LAB}, \cos\theta]$ -plane which are in a close vicinity of a resonance position, (ii) in the near forward direction for $p_{LAB} > 1.6$ GeV/c these zeros trajectories are parallel to $\cos\theta = \mathrm{const}$ etc.

The points of intersections of the $[\mathrm{Im}M_{ij}^{(\pm\kappa)}, \quad \mathrm{Im}Z_{ij}^{(0)}, \quad \mathrm{Im}Z_{ij}^{(\kappa)}]$ -zeros trajectories correspond to the exact degeneracy of the bounds:

$$\lambda(\vec{\kappa}\cdot\vec{P}\sigma) \le 4H \le -\lambda(\sigma) \tag{18}$$

or, equivalently, to the exact saturation of both the bounds (11a). Therefore, in this case from the constraints: $\lambda(\vec{\kappa}\cdot\vec{P}\sigma) = -\lambda(\sigma)$ and the linear equation [in $\vec{\kappa}\cdot\vec{P}$] from table II, we obtain:

$$c_i^2(\vec{\kappa}\cdot\vec{P}_i)\sigma_i = a_{ij} c_j^2\sigma_j(\vec{\kappa}\cdot\vec{P}_j) \pm \{c_i^4\sigma_j^2\xi_{ij}(\vec{\kappa}\cdot\vec{P}_j)^2 - \gamma_{ij}\}^{1/2}, \tag{19a}$$

where

$$a_{ij} \equiv \frac{\lambda(\sigma) + 2c_i^2 c_j^2 \sigma_i \sigma_j}{2c_j^4\sigma_j^2}, \quad \xi_{ij} \equiv a_{ij}^2 - \frac{c_i^4\sigma_i^2}{c_j^4\sigma_j^2},$$

$$\gamma_{ij} \equiv \frac{\lambda(\sigma)}{4c_j^4\sigma_j^2}[c_k^2\sigma_k - c_i^2\sigma_i - c_j^2\sigma_j]^2, \tag{19b}$$

valid for any $i \ne j \ne k = 1,2,3$. Hence, it is of some interest to study in more detail the regions from the $[p_{LAB}, \cos\theta]$ -plane where the bounds (18) for $\vec{\kappa}\cdot\vec{P} = P, T$, S , A and R are nearly degenerated. In order to obtain these regions we define the quantities /13/:

$$F = [1 - 8H/(\sum_{i=+,-,CE} \sigma_i)^2]^{1/2}, \tag{20a}$$

$$F^{(0)} = [1 + 2\lambda(\sigma)/(\sum_{i=+,-,CE} \sigma_i)^2]^{1/2}, \tag{20b}$$

$$F^{(\kappa)} = [1 - 2\lambda(\vec{\kappa}\cdot\vec{P}\sigma)/(\sum_{i=+,-,CE} \sigma_i)^2]^{1/2}, \tag{20c}$$

in terms of which the bounds (18) can be written in the following equivalent form:

$$F^{(0)} \le F \le F^{(\kappa)}. \tag{21}$$

Then, we have used the CERN experimental solutions [7] for phase shifts in order to determine the regions from the $[p_{LAB}, \cos\theta]$ plane where $F - F^{(0)} \le 0.1$ and $F^{(\kappa)} - F \le 0.1$ (or $F^{(\kappa)} - F \le 0.2$). These regions are the unhatched regions presented in figs. 6-10. The intersections of the solid lines [$\mathrm{Im}\,Z_{ij}^{(0)}$ - zeros trajectories] with the dashed lines [$\mathrm{Im}\,Z_{ij}^{(\kappa)}$ -zeros trajectories], also shown in figs. 6-10, correspond to the exact degeneracy of the isospin bounds (18) [or (21)] for $\vec{\kappa}\cdot\vec{P} = P, T, S, A, R,$, respectively. Therefore, in the unhatched regions the bounds (18) are nearly degenerated within the experimental errors [13]. From figs. 6-10 we see that the isospin bounds (18), for $\vec{\kappa}\cdot\vec{P} = P,\ T,\ S$ (A and R) are nearly degenerated: a) in the entire $\cos\theta$ - region for $p_{LAB} < 0.4\,\mathrm{GeV/c}$, b) in the near forward region for $p_{LAB} > 1\ \mathrm{GeV/c}$ and also c) in a close vicinity of $\cos\theta = 0$ for $p_{LAB} > 1\,\mathrm{GeV/c}$ The results presented here are important to choose the regions from $[p_{LAB}, \cos\theta]$-plane where the strong constraints (19a,b) can be tested. Therefore, it would be interesting to test these predictions from the available experimental data.

On the other hand, a problem of great interest in obtaining a test of the possible isospin breaking effects (e.g., indirect effects due to mass and width difference, mixing between π° and η° or between Δ's and N^*'s resonances, etc.) is to know the regions from $[p_{LAB}, \cos\theta]$ -plane where these effects can be observed. Hence, our results (the unhatched regions in figs. 6-10) provide direct information for a localization and

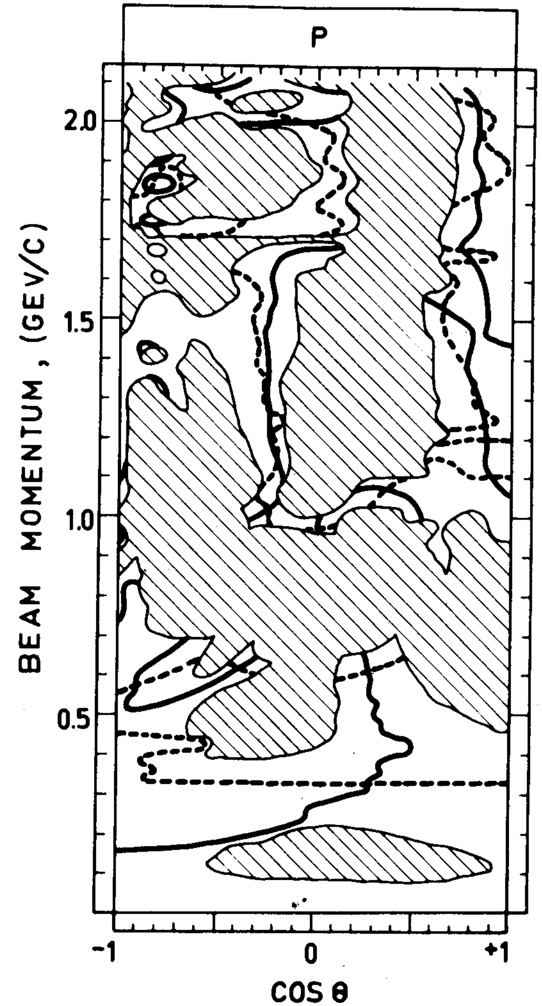

Fig. 6. The degeneracy of the isospin bounds (18) for $\vec{\kappa}\cdot\vec{P} = P$, determined from CERN experimental solutions [7] for πN -phase shifts [see the text] .

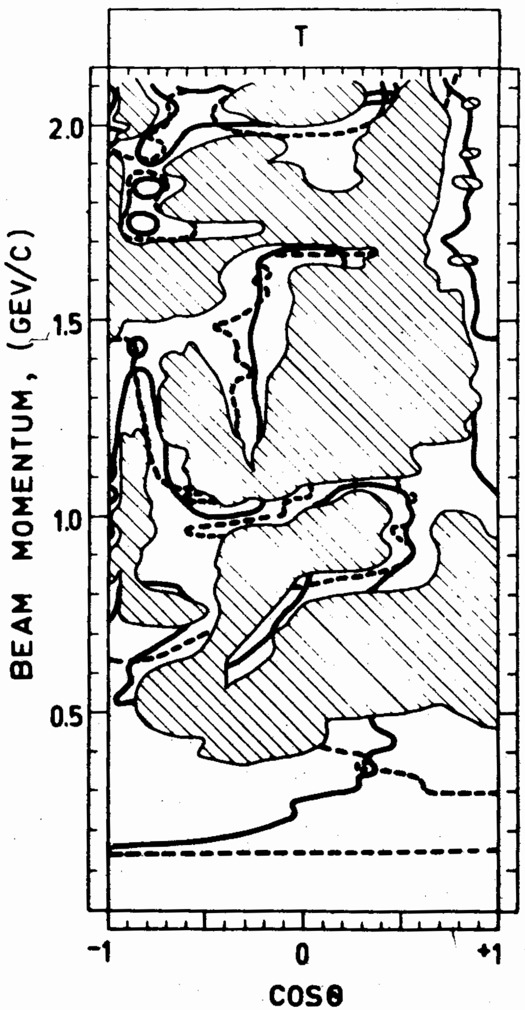

Fig. 7. The degeneracy of the isospin bounds (18) for $\vec{\kappa}\cdot\vec{P} = T$, determined from CERN experimental solutions [7] for πN-phase shifts [see the text].

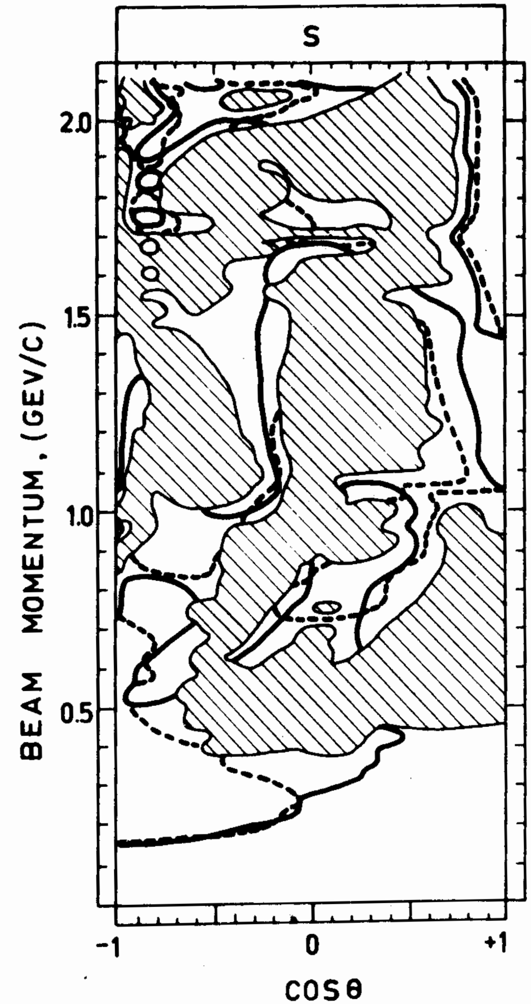

Fig. 8. The degeneracy of the isospin bounds (18) for $\vec{\kappa}\cdot\vec{P} = S$, determined from CERN experimental solutions [7] for πN-phase shifts [see the text].

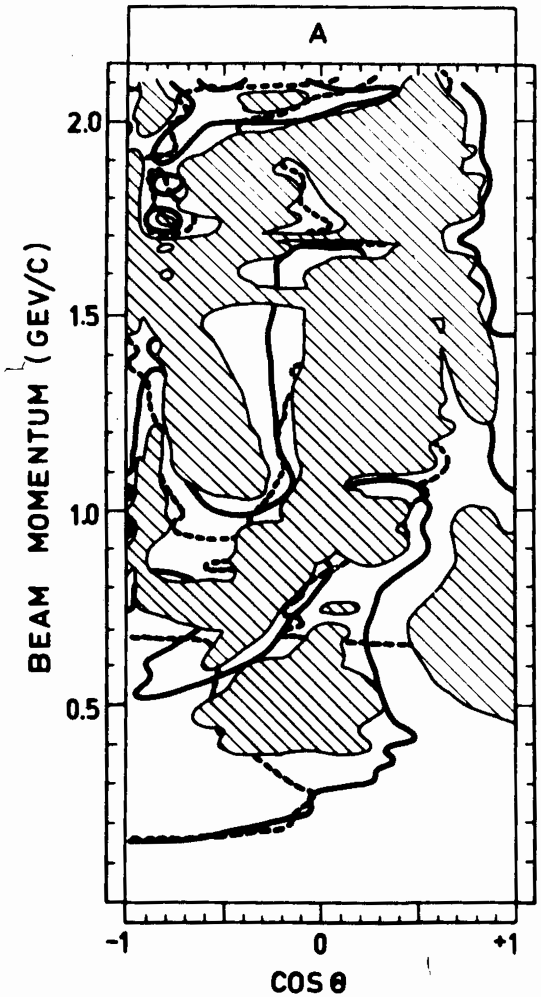

Fig. 9. The degeneracy of the isospin bounds (18) for $\vec{\kappa}\cdot\vec{P} = A$, determined from CERN experimental solutions /7/ for πN -phase shifts [see the text].

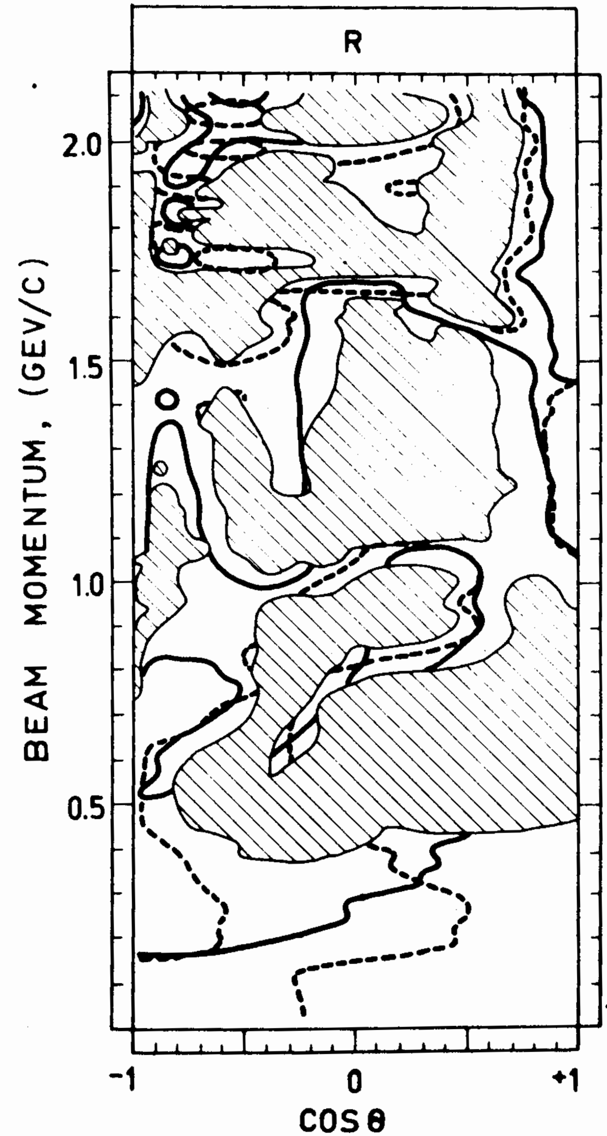

Fig. 10. The degeneracy of the isospin bounds (18) for $\vec{\kappa}\cdot\vec{P} = R$, determined from CERN experimental solutions for πN -phase shifts [see the text].

a detailed investigation of the isospin breaking phenomena.

Next, it is interesting to note that the results in figs. 6-10 are also important for the interpretation of the results /14-15/ since the behaviour of the isospin (ACQN)-distributions can be a consequence of the strong constraints imposed by the isospin invariance and the due to the fact that the saturation or degeneracy of the isospin bounds can be explained by the natural tendency toward conservation of the nucleon (or pion) isospin average quantum parameters. Moreover, the lines from the $[p_{LAB}, \cos\theta]$ plane where the bounds (11b,c) are exactly saturated can be interpreted as lines where $[\langle\vec{\tau}\times\vec{\pi}\rangle_{out}$ and $\langle\vec{\tau}\times\vec{\pi}\otimes\vec{\kappa}\cdot\vec{\sigma}\rangle_{out}$ (resp.)] - isospin average parameters are exactly conserved, since, according to eq. (5) from ref. /15/ , we obtain that these parameters are proportional to $\mathrm{Im}\,Z^{(0)}_{ij}$ and $\mathrm{Im}\,Z^{(\kappa)}_{ij}$, respectively and that

$$\langle\vec{\tau}\times\vec{\pi}\rangle_{in} = \langle\vec{\tau}\times\vec{\pi}\otimes\vec{\kappa}\cdot\vec{\sigma}\rangle_{in} = 0 .$$

[Here, $\vec{\tau}$ and $\vec{\pi}$ are the nucleon and pion isospin operators, (resp.) and $\vec{\sigma}$ are the Pauli matrices] . Therefore, a continuation of figs. 1-10 to higher energies is of great interest for an amplitude analysis and for a phenomenological study of the pion-nucleon scattering. Finally, we remark that the theoretical discussion of the experimental data can be greatly simplified by a simple hypothesis or a specific model on the isospin (ACQN) parameters of inetracting hadrons.

5. Conclusions

We summarize the results as follows.

The exact saturation and the degeneracy of isospin bounds, in terms of the zeros trajectories of $\mathrm{Im}N_{ij}$ [N_{ij} -specific bilinear forms] , are investigated using CERN theoretic /6/ and CERN-experimental /7/ solutions for the pion nucleon phase shifts. So, in sect. 2, all the constraints implied by a triangular relationship (1) are summarized by the equalities (3), (4a,b), (5), (6) [or (8a,b,c)] and the bounds (7a,b,c,d). The introduction of $[M^{(\pm\kappa)}_{ij}, Z^{(0)}_{ij}, Z^{(\kappa)}_{ij}]$ bilinear forms [see eqs. (9a,b,c) from sect 3] allow to discuss the exact saturation of the bounds (11a,b,c) in terms of the $[\mathrm{Im}M^{(\pm\kappa)}_{ij}, \mathrm{Im}\,Z^{(0)}_{ij}, \mathrm{Im}\,Z^{(\kappa)}_{ij}]$ -zeros trajectories or equivalently in terms of $n\pi$ -phase contours. The constraints on experimental data, when the bounds are exactly saturated or degenerated, are given in table II and by eqs. (19a,b), respectively. Next, our results for $[\mathrm{Im}M^{(\pm\kappa)}_{ij}, \mathrm{Im}\,Z^{(0)}_{ij}, \mathrm{Im}\,Z^{(\kappa)}_{ij}]$ -zeros trajectories (ZT), for $\vec{\kappa}\cdot\vec{P} = P, T, S$ (A and R) respectively, are presented in figs. 1-5.

The main reasons to investigate in more detail the (ZT)-topology for the three reactions related by isospin invariance are:

(i) The (ZT)-topology can be determined in a model-independent way by a systematic study of the exact saturation of isospin bounds when accurate experimental data are available;

(ii) The (ZT)-topology is closely related to the strong constraints [see table II and eqs. (19a,b)] imposed by the isospin invariance on the (polarization) experimental data;

(iii) The (ZT)-topology provide a new and unified way of looking at the essential properties of the reactions. They provide a graphic description of those properties which are channel independent (crossing invariant);

(iv) The (ZT)-topology is closely related to the interference and possible isospin breaking phenomena (e.g., mixing between π° and η° or between Δ's and N^*'s , , etc.);

(v) A (ZT)-diagram provides a convenient picture for the comparison of the scattering amplitudes which are obtained from the specific phenomenologic models or by different asymptotic assumptions. The (ZT)-diagrams can be used in the development and comparison of phase shift solutions for scattering amplitudes and permit a rapid identification of such features as zeros of the scattering amplitudes in the physical region;

(vi) The (ZT)-diagrams can be used as a guide in developing a unified phenomenological theory that includes all transfer momenta both in the resonance region and in high energy regions;

(vii) The (ZT)-topology is important for the interpretation of experiments in terms of the exact conservation of a specific (ACQN) isospin and

isospin-spin polarization parameters [see sect. 3 and refs.[14-15]], etc.

Next, our results on the analysis of degeneracy of isospin bounds (18), for $\vec{\kappa}\cdot\vec{P} = P,T,S$ (A and R) respectively, are given in figs. 6-10, These results are important for experimental test of the strong constraints (19a,b) and also for test and detailed investigation of the isospin breaking phenomena which are expected to be observed in the unhatched regions of figs. 6-10. We note that apparent isospin breaking effects are also expected to be present in these regions because the methods to calculate electromagnetic corrections are not yet adequate. Therefore the effects of this type will be important for an improvement of theoretical treatment of Coulomb interference phenomena, electromagnetic corrections of resonance parameters, etc. Hence, it would be interesting to test the equalities (3), (4a,b), (5), (6) [or (8a,b,c)] in the unhatched regions from figs. 6-10 and to determine the breaking parameters in a model-independent way [see ref.[16]].)

Finally, we remark that in order to develop an intuition based on the (ZT)-topology [or exact conservation of the (ACQN) isospin and isospin-spin polarization parameters] it is first necessary to obtain (ZT)-topologies for other reactions (e.g., those given in table I) and to derive their characteristics features from different special models.

References

1. M.G.Doncel,L.Michel and P.Minnaert. Phys.Lett., 38B, 42 (1972).
2. D.B.Ion, Nuclear Phys., B84, 55 (1975) and JINR preprints: E2-7732, E2-7868, Dubna, 1974.
3. D.B.Ion. JINR preprint, E2-8213, Dubna, 1974.
4. D.B.Ion. JINR preprint, E2-8695, Dubna, 1975.
5. D.B.Ion. JINR preprints E2-8865-66, Dubna, 1975.
6. D.J.Herndon, A.Barbaro-Galtieri and A.Rosenfeld. πN- partial-wave amplitudes, Particle Data Group, compilation, UCRL-20030 (1970).
7. S.Almehed, C.Lovelace. CERN, TH-1403 and Nucl.Phys., B40, 157 (1972).
8. M.Gourdin. Unitary Symmetries (North-Holland Amsterdam, (1967).
9. R.Chand. Phys.Rev., D9, 2056 (1974).
10. J.Ervane, M.Korkea-aho and N.A.Tornqvist "The Puzzle of the Near-Saturation of Isospin Bounds in $\pi N \to \pi N$, $KN \to KN$ and $\pi N \to K\Sigma$ ", preprint Helsinki 23-74 (1974).
11. L.Michel. Nuovo Cimento, 22, 203 (1961).
12. R.J.N.Phillips. Nuovo Cimento, 26, 103 (1962).
13. D.B.Ion, F.G.Nichitiu, A.C.Mihul. JINR Preprint E2-7961, Dubna, 1974.
14. D.B.Ion, A.C.Mihul. Annals of Phys., 93, (1975) and JINR preprint E2-7733, Dubna, 1974.

15. D.B.Ion, A.C.Mihul. Annals of Phys., 93 (1975), and JINR preprint E2-7734, Dubna, 1974.
16. D.B.Ion. Nucl.Phys. B96, 67 (1975) and JINR preprint E2-8432, Dubna, 1974.

Received by Publishing Department
on August 25, 1975.